nature astronomy

Article

https://doi.org/10.1038/s41550-024-02254-3

In situ observation of mass ejections caused by magnetic reconnections in the ionosphere of Mars

Received: 5 March 2023

Accepted: 21 March 2024

Published online: 22 April 2024

Check for updates

Yudong Ye[1,2], Xiaojun Xu[1] ✉, Lou-Chuang Lee[3] ✉, Jiang Yu[2], Jing Wang[2], Bei Zhu[4], Qing Chang[5], Jiaying Xu[6], Qi Xu[7] & Zilu Zhou[1]

Explosive mass ejections triggered by magnetic activities are common on our Sun and other stars in the Universe. However, there is a lack of evidence for such explosive phenomena in magnetized or partially magnetized planets with atmospheres. Here we present direct evidence for explosive mass ejections from the Martian ionosphere, resulting from magnetic reconnections between strong crustal field regions with open magnetic fields. A plasma density cavity with signatures of magnetic reconnection that is directly evident for an eruptive mass ejection caught in the act indicates that a considerable amount of ionospheric mass has been rapidly ejected into space. Although Martian mass loss associated with magnetic reconnection has been reported previously, our results demonstrate that explosive mass ejections can occur even on partially magnetized planets without global magnetic fields. In this scenario, we suggest that strong localized magnetic fields extending above the exobase are needed.

In the corona of the Sun and Sun-like stars, explosive coronal mass ejections (CMEs) remove giant mass from the stars[1–3]. The plasma environment in the Martian ionosphere, especially above strong crustal fields[4], is similar to that in the solar corona. Both regions have complex magnetic topologies[5–8] and very low plasma beta[9,10], creating favourable conditions for the occurrence of magnetic reconnection. Consequently, eruptive mass depletions are anticipated to take place. Previous studies have demonstrated the frequent occurrence of quasi-steady magnetic reconnection in the Martian induced magnetosphere[11–14] as well as in the ionosphere[15] and proposed that magnetic reconnection could lead to ion loss on Mars and bulk plasma escape[16–24]. However, direct evidence of bulk plasma escape resulting from magnetic reconnection, especially mass ejections, in the ionosphere of Mars is still absent.

The observational characteristics of CMEs and mass ejections from the ionosphere are expected to differ. Unlike CMEs, the mass ejected into space from Mars may not be dense enough to scatter sunlight and create a white light bubble. As a result, a direct indication of a mass ejection could be the presence of a density cavity in the ionosphere. In this Article, we examine Mars Atmosphere and Volatile EvolutioN (MAVEN)[25] data and identified three density cavities associated with magnetic reconnection in the dayside ionosphere on 18 October 2014, 19 December 2016 and 19 April 2019. While all these events exhibited nearly identical observational characteristics, we present only the analysis for the event on 19 October 2016 (Fig. 1). The analyses for the events on 18 October 2014 and 19 April 2019 are provided in Supplementary Figs. 1–4.

[1]State Key Laboratory of Lunar and Planetary Sciences, Macau University of Science and Technology, Taipa, People's Republic of China. [2]Planetary Environmental and Astrobiological Research Laboratory, School of Atmospheric Sciences, Sun Yat-sen University, Zhuhai, People's Republic of China. [3]Institute of Earth Science, Academia Sinica, Nankang, Taiwan. [4]Space Engineering University, Beijing, People's Republic of China. [5]Shandong Institute of Advanced Technology, Jinan, People's Republic of China. [6]Research Center for Intelligent Computing Platforms, Zhejiang Laboratory, Hangzhou, People's Republic of China. [7]State Key Laboratory of Space Weather, National Space Science Center, Chinese Academy of Sciences, Beijing, People's Republic of China. ✉e-mail: xjxu@must.edu.mo; louclee@earth.sinica.edu.tw

https://doi.org/10.1038/s41550-024-02254-3

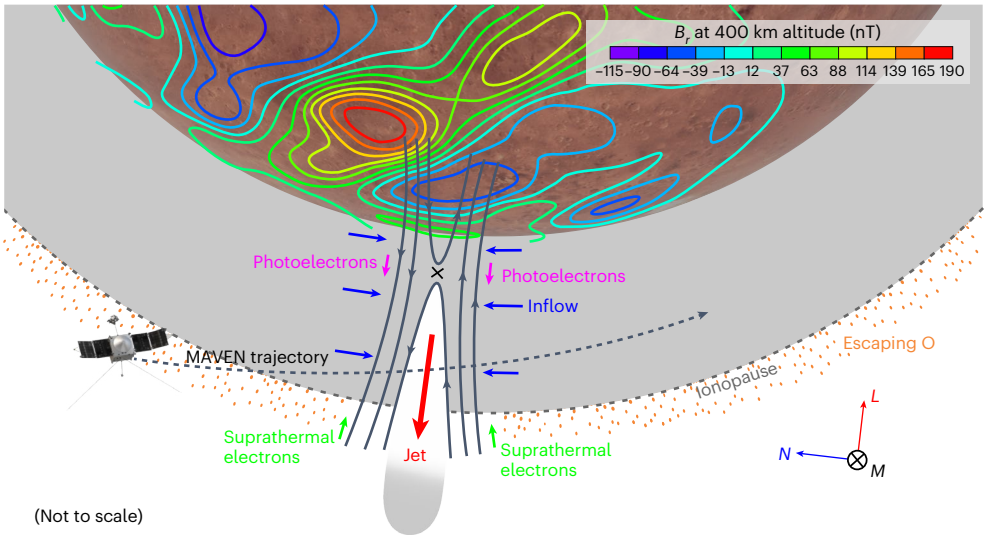

Fig. 1 | A diagram of MAVEN crossing a plasma cavity within a reconnection exhaust after a mass ejection in the dayside ionosphere. The magnetic field lines are illustrated in the local current sheet coordinates (the *LMN* coordinates, with *L* along the exhaust, *M* along the *X* line and *N* perpendicular to the current sheet). Coloured contours on the Martian topographic map represent the radial component (B_r, positive outwards) of crustal magnetic fields at 400 km altitude[26]. The magnetic reconnection exhaust was located between opposing open magnetic fields above two strong crustal field regions with different polarities. MAVEN's trajectory is shown by a dashed line, arrowed for direction. The grey-colored zone signifies the Martian ionosphere, abundant with heavy ions. The outflow jet was along the −*L* direction, moving outwards from Mars into space. Suprathermal electrons from the solar wind were moving towards Mars, and photoelectrons from the ionosphere were moving outwards along these open magnetic field lines.

Results

On 19 October 2016, MAVEN crossed a magnetic reconnection exhaust between 20:50:57 and 20:52:29 universal time (UT). MAVEN was approaching the periapsis of orbit 4,002 with an altitude decreasing from 732.7 to 638.3 km. During this period, the solar zenith angle (SZA) changed from 58° to 56°, suggesting that MAVEN was on the dayside. Magnetic reconnection signals associated with the exhaust include a dip in the magnetic field strength corresponding to the magnetic field rotation (Fig. 2b), a plasma jet indicated by enhancements in the ion velocities (Fig. 2d), and electron heating and O_2^+ heating as revealed by the energy spectra in Fig. 2e and 2f, respectively. Crustal magnetic fields from the Morschhauser model[26] are provided as a reference in Fig. 2c, which should contribute substantially to the observed magnetic fields. Here, we only show the O_2^+ energy spectrum as O_2^+ is the primary composition. The ion energy spectra of other heavy ions are similar. The mass spectrum shown in Fig. 2g confirms that MAVEN was in the ionosphere, where the dominant ion species are heavy ions. Considering the notably low flux of H^+ as shown in Fig. 2g, only the heavy ions are analysed.

Magnetic reconnection analysis

To obtain the exhaust outflow orientation, the local current sheet (*LMN*) coordinates were determined by applying minimum variance analysis to the magnetic field data across the current sheet[27,28]. The eigenvalue ratio λ_2/λ_3 (intermediate to minimum) is 4.39, much greater than unity, indicating the reliability of the calculated normal direction. It is worth noting that there is no evidence of a reconnection-associated Hall magnetic field in this case. Consequently, the reconnection exhaust encountered by MAVEN was located relatively far from the reconnection site rather than within the ion diffusion region. The outflow jet was observed in the *L* direction, corresponding to $(-0.13\hat{x}, -0.35\hat{y}, -0.93\hat{z})$ in Mars Solar Orbital (MSO) coordinates, where *X* points from Mars to the Sun, *Y* is opposite to Mars's orbital velocity and *Z* is perpendicular to the orbital plane. Since the exhaust was in the Southern Hemisphere, the outflow jet primarily followed the MSO −*Z* direction, moving outwards from Mars into space. The reconnection jet exhibited maximum velocities ranging from 14 to 23 km s^{-1} for various ions, which are sufficiently high for these ions to escape Mars. However, the inflow speeds of the ions are exceptionally low. The inflow speed can be determined from the shift in V_N across the reconnection exhaust (Fig. 3d). For each heavy ion composition, the difference in V_N across the exhaust corresponds to a (mass-weighted) local inflow velocity of ~0.35 km s^{-1}. The inflow conditions at different altitudes can vary considerably, and the Alfvén speed in the inflow region is difficult to estimate since MAVEN did not encounter the reconnection site.

Magnetic topology analysis

Magnetic topology is important for understanding the mechanism of magnetic reconnection that could trigger a mass ejection in the ionosphere. Measurements of suprathermal electrons[29,30] and shape parameters[31,32] have been widely used to determine magnetic topology. Figure 4a presents the pitch angle distributions of electrons with energies ranging from 111 to 140 eV. Clear loss cones can be observed in the parallel (to the magnetic field) and antiparallel directions in the leading and trailing ambient regions, respectively. Such one-sided loss cones in suprathermal electron distributions indicate that the associated magnetic fields are open[29]. Within the reconnection exhaust, suprathermal electrons were moving in both parallel and antiparallel directions, revealing that the magnetic field lines in the exhaust have both ends connected to the solar wind magnetic field. Figure 4b shows the calculated dimensionless shape parameters, with values well above 1 indicating the presence of solar wind electrons and those well below 1 indicating the presence of ionospheric electrons[31,32]. Although the shape parameters being near 1 bring some ambiguity, the presence of open magnetic fields can be confirmed by electron energy spectra at two time positions marked by the thick vertical dashed lines labelled by 'c' and 'f' in Fig. 4a,b: ionospheric photoelectrons were only observed in one direction (Fig. 4c,f). The fact that both shape parameters are well above 1 within the reconnection exhaust indicates that the magnetic field lines are connected to the solar wind magnetic field at both ends. Detailed electron energy spectra (Fig. 4d,e) within the exhaust further confirm that electrons in both parallel and antiparallel directions are solar wind electrons. Hence, these results are consistent with those obtained from suprathermal electrons in Fig. 4a. A possible driver

for the mass ejection caused by the reconnection between open crustal magnetic field lines could be a change of the solar wind dynamic pressure, as suggested in previous studies[12]. Because of the complex magnetic polarities, the crustal fields on the dayside can reconnect with the interplanetary magnetic field of any polarity, resulting in open magnetic field lines. Dynamic pressure changes in the solar wind can further trigger magnetic reconnection between these open magnetic field lines, resulting in the recovery of the crustal field and the formation of the mass ejection at Mars. This process is illustrated in Supplementary Fig. 5.

Ejected mass estimation

A mass ejection event in the ionosphere could eject a notable amount of ionospheric mass into space. On the basis of the ion density variations shown in Fig. 3f, the total oxygen (O) ion loss from O^+, O_2^+ and CO_2^+ for this mass ejection event can be estimated by assuming that 99% of the ionospheric plasma in the volume of the reconnection exhaust, from an altitude of ~300 km to the ionopause, is ejected. This assumption is made owing to the considerable reduction in the magnetic reconnection rate below 300 km caused by ion-neutral collisions[10]. For simplicity, the tilt of the exhaust in relation to the vertical direction is ignored in the calculation. We consider that the reconnection *X* line spanned 550 km, corresponding to a 15° span in longitude between the oppositely directed crustal fields as illustrated in Fig. 2a. After correcting for the satellite's velocity, the exhaust width is calculated to be 132 km on the basis of MAVEN measurements. By utilizing the ion densities measured by MAVEN during this orbit, which has a periapsis altitude of 179 km around 55° SZA, the integrated O ion loss is estimated to be approximately 1.3 kg for this mass ejection event. Considering that it takes about 20 s for the ionospheric plasma to be ejected from the potential reconnection site (about 300 km in altitude) to MAVEN's altitude (roughly 700 km) through the jet with a velocity of 20 km s^{-1}, this single mass ejection event can temporarily increase the ion loss by a rate of 2.4×10^{24} s^{-1}, which is comparable to the global O ion loss rate[22].

Discussion

MAVEN's encounter with the reconnection exhaust in the southern ionosphere of Mars can be summarized as shown in Fig. 1. When MAVEN crossed the boundary region between two strong crustal fields with opposite polarities, it initially entered the leading inflow region, where the magnetic field lines were open and pointing outwards (mainly in the $-L$ direction as shown in Fig. 3a). Consequently, suprathermal electrons from the solar wind exhibited a loss cone in the parallel direction (Fig. 4a) and ionospheric electrons moved outwards in the parallel direction (Fig. 4c). The situation in the trailing inflow region is similar, except that the magnetic field was generally along the $+L$ direction. As a result, the suprathermal electron loss cone and ionospheric electrons were in the antiparallel direction (Fig. 4a,f). Within the exhaust, reconnected magnetic field lines have both ends connected to the solar wind. As a large amount of ionospheric plasma was already ejected by the reconnection, a plasma cavity was left without being efficiently refilled by the ambient plasma. The reconnection jet, with a velocity of approximately 20 km s^{-1}, can rapidly eject the ionospheric plasma from ~300 km into space within 30 s at the very beginning of the magnetic reconnection when the reconnecting plasma is dense, indicating an explosive ejection. After most of the plasma around the reconnection site has been ejected, much less ionospheric plasma participated in the reconnection.

The entire process can be indicated by the fact that the reconnection outflow density within the density cavity is two orders of magnitude less than the background plasma density measured by MAVEN both before and after the density cavity. Theoretically, the outflow density is close to or slightly larger than the inflow density[33], which has been proved by observations in Earth's magnetopause[34], magnetotail[35] and solar wind[36] reconnections. At the beginning of reconnection, the inflow density is the background plasma density near the reconnection site. As a result, a substantial portion of the ionospheric mass in proximity to the reconnection site could be ejected, leading to the formation of a mass ejection event. Afterwards, much less plasma is involved in the reconnection, causing the outflow density observed in the density cavity to decrease markedly. Under the condition of very low plasma beta, the ambient plasma cannot cross the open magnetic fields to sufficiently refill the density cavity[37] created by the mass ejection. Furthermore, the magnetic reconnection in the ionosphere can be kept continuously ongoing after a mass ejection, as observed by MAVEN.

Previous studies have suggested that magnetic reconnection can lead to ion loss of Mars. Recent observations have also confirmed that the magnetic reconnection at the induced magnetopause[23] and the magnetosheath[24] can directly remove ionospheric mass. It is important to note, however, that the previously detected magnetic reconnection events have all been of a quasi-steady nature. For the first time, our results demonstrate that explosive mass ejections in the ionosphere, similar to CMEs, can take place in the ionosphere of Mars, contributing to the ion loss there. While there have been studies highlighting the similarities between the reconnection features associated with CMEs and magnetotail plasmoids[38,39], it should be noted that the reconnection-triggered mass ejections in the ionosphere and CMEs are substantially different from the plasmoids in the magnetotail in producing atmospheric loss. This distinction arises from the fact that particles within magnetotail plasmoids have already escaped from the planet.

The presence of a density cavity associated with reconnection provides compelling evidence for a mass ejection event on Mars. The estimated total amount of lost oxygen ions resulting from the aforementioned mass ejection event is up to 1.3 kg. Furthermore, a survey of MAVEN data reveals an approximate occurrence rate of three mass ejection events per Martian day (Sol). These findings collectively indicate that the cumulative loss of oxygen ions owing to mass ejections over the course of 4.2 billion years is roughly equivalent to a layer of water approximately 0.046 mm deep covering the planet's surface, assuming all the oxygen originates from water. Considering that the occurrence is probably much higher than estimated, mass ejection events can partially contribute to the ion loss from Mars, particularly during the early stages of the Solar System when the solar wind was stronger. Our findings demonstrate that the phenomenon of explosive mass ejections can occur on Mars-like planets with an atmosphere and crustal fields, in addition to stars. As a result of explosive mass ejections from

Fig. 2 | MAVEN trajectory overview and selected measurements near the reconnection exhaust. a, The MAVEN orbit projected onto the surface of Mars in geographic coordinates, overlaid with crustal magnetic fields. **b**, The measured magnetic fields (*B*) in MSO coordinates. **c**, The crustal magnetic fields in MSO coordinates given by Morschhauser's model. **d**, The ion bulk velocities measured by MAVEN/STATIC (hereafter, STATIC) instrument. **e**, The electron energy spectrum measured by MAVEN/SWEA (hereafter, SWEA) instrument. **f**,**g**, The energy spectrum of O_2^+ (EO_2^+) (**f**) and the mass spectrum measured by STATIC (**g**) with an apparent flux cavity. The dashed black lines on the projected MAVEN trajectory in **a** mark the exhaust boundaries' time positions, aligned with vertical dashed lines in **b**–**g**. The white asterisk symbol in **a** marks the subsolar point at 20:52:00 UT, and the curve of diamonds represents the terminator at the same time. MAVEN's altitude is colour-coded on its trajectory, with a reference colour bar in the top right. Ion bulk velocities outside the exhaust are plotted as dashed lines, as velocities in low ion-energy regions may include the spacecraft ram effect. However, the ion velocities should be lower than the escape speed of Mars (5 km s^{-1}), preserving accurate reconnection jet identification. Clear magnetic reconnection signals associated with a plasma density cavity are observed. All spectral fluxes are measured as energy fluxes (Eflux) in units of eV cm^{-2} s^{-1} sr^{-1} eV^{-1}.

https://doi.org/10.1038/s41550-024-02254-3

the ionosphere and quasi-steady ion and atom escapes, such planets lose mass in a quite similar manner to our Sun through explosive CMEs and the quasi-steady solar wind.

Given the explosive and distinctive characteristics of the mass ejection caused by reconnection in the low-beta ionosphere of Mars-like planets, which differ from previous reconnection observations, we

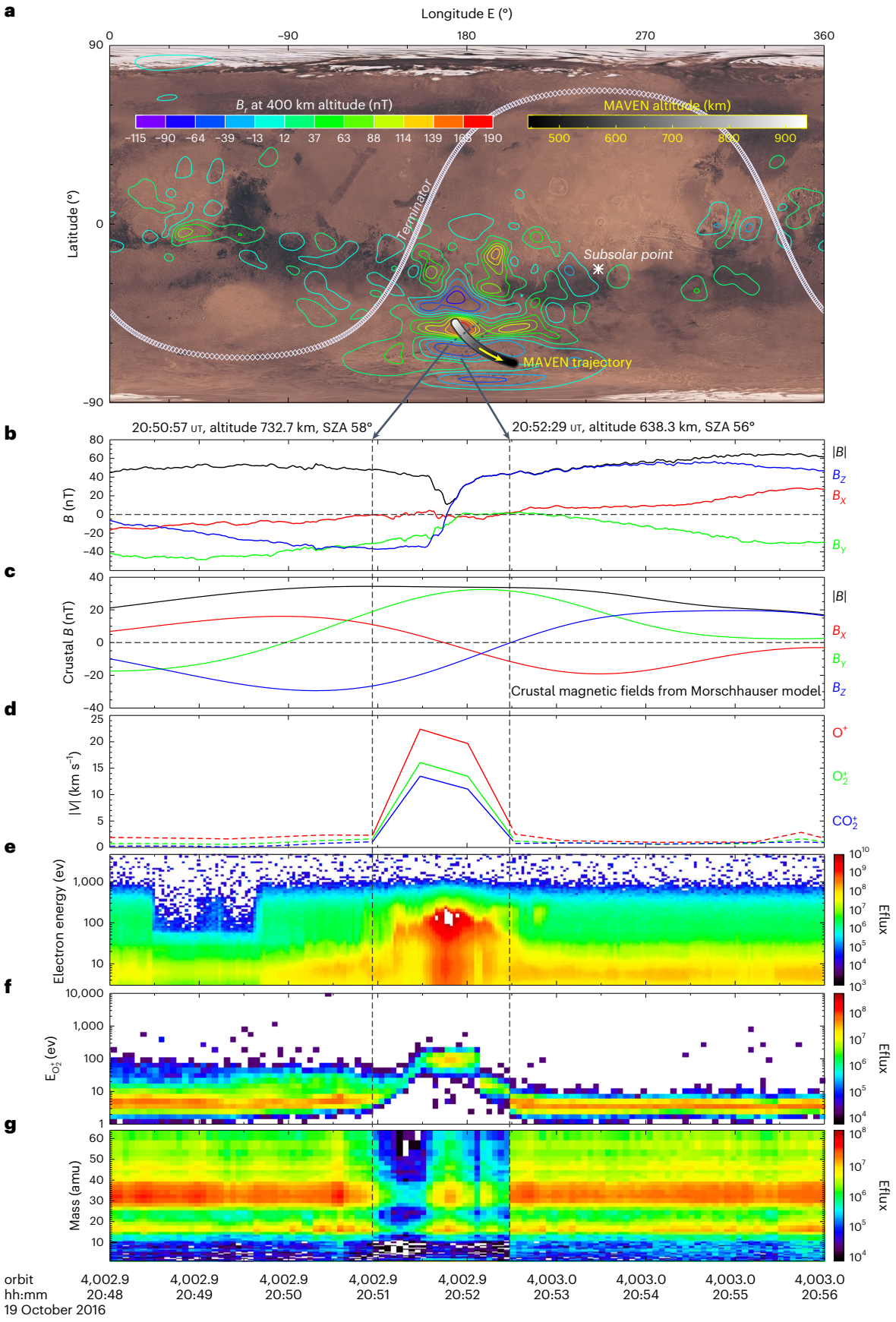

https://doi.org/10.1038/s41550-024-02254-3

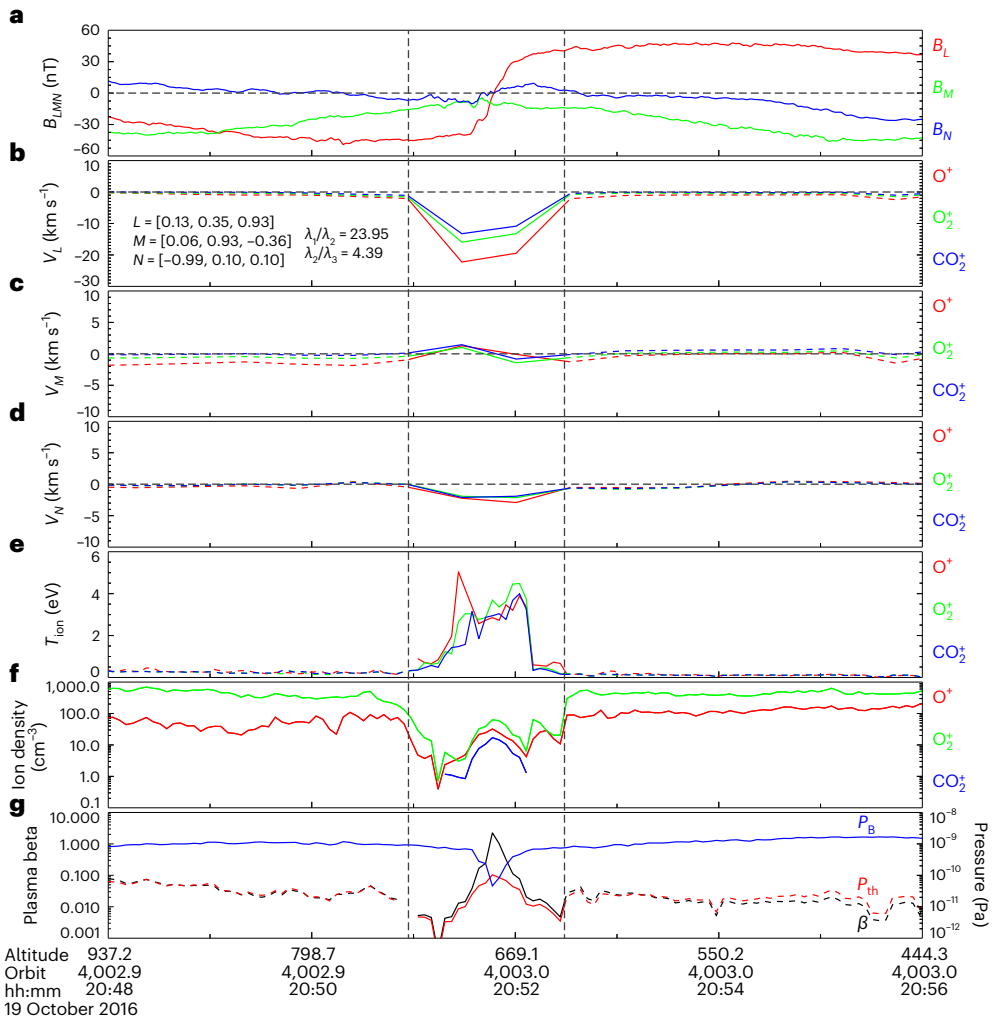

Fig. 3 | Further evidence for magnetic reconnection in association with the plasma cavity. a, The magnetic fields in *LMN* coordinates. **b**–**d**, The V_L (**b**), V_M (**c**), and V_N (**d**) components of different ions measured by STATIC. **e**, The ion temperatures. **f**, The ion densities. **g**, The plasma beta, magnetic pressure (P_B) and thermal pressure (P_{th}). The dashed lines are positioned as in Fig. 2. The *L*, *M*, and *N* directions in MSO coordinates as well as the ratios of the maximum to intermediate and intermediate to minimum variances are given in **b**. The ion jet and heating accompanying the magnetic strength dip clearly indicate magnetic reconnection. The reconnection jet is along the −*L* direction, with the outflow plasma in the Southern Hemisphere primarily moving in the −*Z* MSO direction, indicating outward movement. The densities of O_2^+ and other heavy ions decreased by nearly two orders of magnitude within the reconnection exhaust, implying extensive plasma ejection into space and resulting in an ionospheric plasma cavity. The surrounding regions exhibit a low plasma beta. The reconnection site, at a lower altitude, has a stronger crustal field, further reducing the plasma beta and promoting magnetic reconnection.

propose to refer to this process as ionospheric mass ejections (IMEs), drawing a parallel with CMEs. However, to avoid potential confusion, it is important to emphasize that IMEs, which result from open magnetic field reconnection, follow a different mechanism than CMEs, which result from filament eruptions. The energy inputs for CMEs and IMEs are also distinct: the energy released by CMEs originates from the lower atmosphere of the Sun, while the energy released by Martian IMEs comes from the solar wind.

Methods

MAVEN data survey

To identify potential mass ejections in MAVEN measurements, the following criteria were applied: MAVEN is in the dayside of Mars (SZA of ≤90°), MAVEN is above a selected strong crustal magnetic field region with longitude ranging from 90° E to 270° E and latitudes spanning from 90° S to 30° N in Martian geological coordinates (Supplementary Fig. 6). These criteria allowed us to automatically identify 9,322 data segments. Subsequently, each segment was manually examined for magnetic reconnection signatures, along with the presence of a cavity containing heavy ionospheric ions. As a result of this analysis, three mass ejection events, occurring on 18 October 2014, 19 December 2016, and 19 April 2019, were identified.

Quantifying the cumulative ion loss by mass ejections from the ionosphere

Using only a single satellite's observations, we can provide a rough estimate of the total ion loss caused by mass ejections. Given that only one detector is involved, our estimation is highly constrained. However, the extensive coverage of MAVEN trajectories in the Martian ionosphere lends credibility to our estimation.

From the filtered data segments mentioned in the previous section, we conducted a search for periods when MAVEN was in an environment with abundant heavy ions (with the number density of O_2^+ greater than 1,000 cm^{-3}) and low plasma beta ($\beta < 0.1$). Under these conditions, MAVEN is capable of detecting density cavities, as the ionospheric plasma is unable to adequately refill the cavities left by mass ejections. In our data segments, the total flight time that meets these criteria is approximately 6,593 min, during which we identified three mass

https://doi.org/10.1038/s41550-024-02254-3

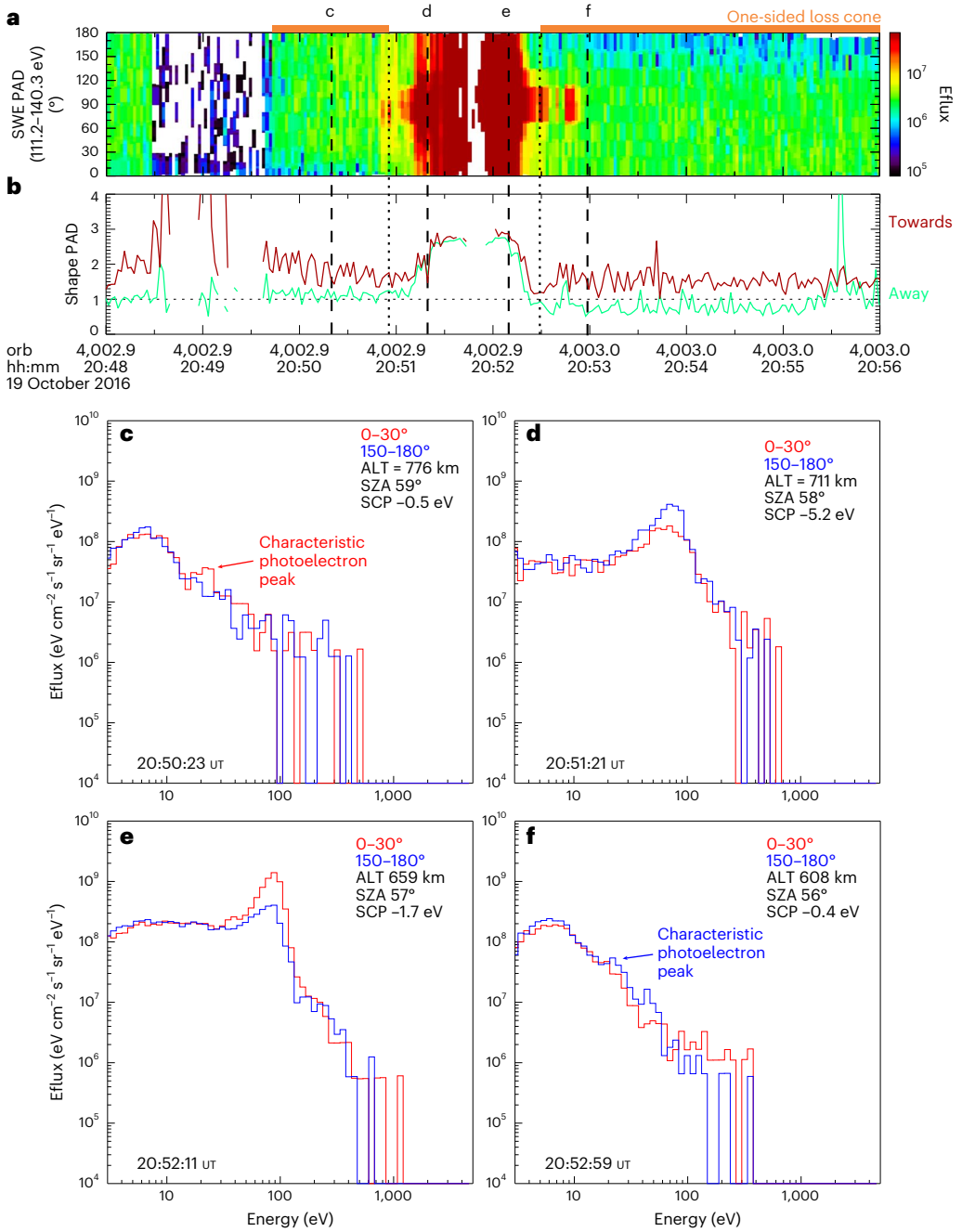

Fig. 4 | Magnetic topology analysis using suprathermal electron measurements and the shape parameter. a, The pitch angle distribution from SWEA measurements (SWE PAD) of 111–140 eV electrons. **b**, The shape parameters for electrons moving towards (red) and away from (green) the planet. The vertical dashed lines are positioned as in Figs. 2 and 3, marking the exhaust boundaries. **c**–**f**, The electron energy spectra in parallel (0–30°) and antiparallel (150–180°) directions at times indicated by the thick vertical dashed lines labelled 'c' (**c**), 'd' (**d**), 'e' (**e**) and 'f' (**f**) in **a** and **b**. ALT, altitude; SCP, spacecraft potential estimated by SWEA. The one-sided loss cone outside the exhaust region in **a** (orange bars at top) suggests open magnetic field lines[29]. A characteristic photoelectron peak[44] can be identified in the parallel spectrum at 20:50:23 UT in **c** and in the antiparallel spectrum at 20:52:59 UT in **f**, while the electron spectra in the opposite directions show no photoelectron signals. The 20:51:21 UT electron spectra in **d** and the 20:52:11 UT electron spectra in **e**, in both parallel and antiparallel directions, show typical features of solar wind electrons, suggesting that magnetic field lines in the exhaust connect to the solar wind at both ends.

ejection events. These density cavities are attributed to magnetic reconnection between open magnetic field lines of opposite polarities. Therefore, regions where a single magnetic polarity dominates (which account for about four-fifths of the total strong crustal field area) should not be considered.

Assuming that the 6,593 min are evenly distributed across the strong crustal field area, it is reasonable to expect that the MAVEN instrument can detect a single mass ejection event approximately every 440 min above the boundary regions between crustal fields with opposite polarities. These boundary regions account for about one-fifth of the total strong crustal field area. The occurrence rate is one mass ejection event every 440 min. This was calculated by first dividing the total duration of 6,593 min by 5 and then further dividing that result by the three events. Considering that the selected strong magnetic field region persists for about 11 h (or 660 min) on the dayside, the occurrence rate is thus estimated to be 1.5 (=1/440 × 660) mass ejections per Martian day (Sol). This occurrence rate could potentially double to three mass ejections per Sol if we take into account the global

crustal magnetic field on Mars. Since the interplanetary magnetic field can reconnect with various sections of the crustal fields in the dayside ionosphere and the crustal fields eventually recover on the nightside, it is plausible to anticipate that mass ejections from the ionosphere could occur three times per Martian day (Sol) across the widely distributed crustal fields on Mars.

Assuming an average mass loss of 1.3 kg of oxygen ions in a mass ejection event, the total oxygen ion loss over 4.2 billion years would amount to approximately 6×10^{12} kg. If we consider all this oxygen to have originated from H_2O and distribute it uniformly across Mars's surface, it would correspond to a global water layer of 0.05 mm. Compared with a water layer of 0.2 m thickness, deduced from the current global oxygen ion loss rate, such mass ejections contribute approximately 0.25‰. However, the occurrence rate of mass ejections should be higher owing to the transient nature of these phenomena. Mass ejections with already refilled density cavities cannot be detected, resulting in a narrow detection window. Moreover, the strong solar wind conditions that were prevalent in the early stage of the Solar System can produce more open magnetic field lines and thus increase the occurrence rate of mass ejections.

Data availability

The MAVEN data used to generate the plots are available via the Planetary Data System at https://pds.nasa.gov (ref. 40) or the MAVEN Science Data Center at https://lasp.colorado.edu/maven/sdc/public/ (ref. 41).

Code availability

Codes for this study are available via GitHub at https://github.com/StellarPlasma/MAVEN_IDL (ref. 42), written based on Space Physics Environment Data Analysis Software, which can be downloaded via spedas.org at http://spedas.org/wiki/index.php?title=Downloads_and_Installation (ref. 43).

References

1. Gopalswamy, N. History and development of coronal mass ejections as a key player in solar terrestrial relationship. *Geosci. Lett.* **3**, 1–18 (2016).
2. Chen, J. Coronal mass ejections: causes and consequences—a theoretical view. *Geophys. Monogr. Ser.* **99**, 65–81 (1997).
3. Chen, P. F. Coronal mass ejections: models and their observational basis. *Living Rev. Sol. Phys.* **8**, 1–92 (2011).
4. Connerney, J. E. et al. Tectonic implications of Mars crustal magnetism. *Proc. Natl Acad. Sci. USA* **102**, 14970–14975 (2005).
5. Bougher, S. W., Cravens, T. E., Grebowsky, J. & Luhmann, J. The aeronomy of mars: characterization by MAVEN of the upper atmosphere reservoir that regulates volatile escape. *Space Sci. Rev.* **195**, 423–456 (2015).
6. Mitchell, D. L. et al. Probing Mars' crustal magnetic field and ionosphere with the MGS Electron Reflectometer. *J. Geophys. Res.* **106**, 23419–23427 (2001).
7. Matta, M., Mendillo, M., Withers, P. & Morgan, D. Interpreting Mars ionospheric anomalies over crustal magnetic field regions using a 2-D ionospheric model. *J. Geophys. Res. Space Phys.* **120**, 766–777 (2015).
8. Xu, S. et al. High-altitude closed magnetic loops at Mars observed by MAVEN. *Geophys. Res. Lett.* **44**, 211,229–211,238 (2017).
9. Hanson, W. B. & Mantas, G. P. Viking electron temperature measurements: evidence for a magnetic field in the Martian ionosphere. *J. Geophys. Res. Space Phys.* **93**, 7538–7544 (1988).
10. Cravens, T. E. et al. Magnetic reconnection in the ionosphere of Mars: the role of collisions. *J. Geophys. Res. Space Phys.* **125**, e2020JA028036 (2020).
11. Eastwood, J. P. et al. Evidence for collisionless magnetic reconnection at Mars. *Geophys. Res. Lett.* **35**, L02106 (2008).
12. Halekas, J. S. et al. In situ observations of reconnection Hall magnetic fields at Mars: evidence for ion diffusion region encounters. *J. Geophys. Res.* **114**, A11204 (2009).
13. Harada, Y. et al. Magnetic reconnection in the near-Mars magnetotail: MAVEN observations. *Geophys. Res. Lett.* **42**, 8838–8845 (2015).
14. Harada, Y. et al. Survey of magnetic reconnection signatures in the Martian magnetotail with MAVEN. *J. Geophys. Res. Space Phys.* **122**, 5114–5131 (2017).
15. Harada, Y. et al. Magnetic reconnection on dayside crustal magnetic fields at Mars: MAVEN observations. *Geophys. Res. Lett.* **45**, 4550–4558 (2018).
16. Brain, D. A. et al. Episodic detachment of Martian crustal magnetic fields leading to bulk atmospheric plasma escape. *Geophys. Res. Lett.* **37**, L14108 (2010).
17. Brain, D. et al. A comparison of global models for the solar wind interaction with Mars. *Icarus* **206**, 139–151 (2010).
18. Brain, D. A., Hurley, D. & Combi, M. R. The solar wind interaction with Mars: recent progress and future directions. *Icarus* **206**, 1–4 (2010).
19. Hara, T. et al. Formation processes of flux ropes downstream from Martian crustal magnetic fields inferred from Grad–Shafranov reconstruction. *J. Geophys. Res. Space Phys.* **119**, 7947–7962 (2014).
20. Lillis, R. J. et al. Characterizing atmospheric escape from Mars today and through time, with MAVEN. *Space Sci. Rev.* **195**, 357–422 (2015).
21. Hara, T. et al. MAVEN observations of a giant ionospheric flux rope near Mars resulting from interaction between the crustal and interplanetary draped magnetic fields. *J. Geophys. Res. Space Phys.* **122**, 828–842 (2017).
22. Jakosky, B. M. et al. Loss of the Martian atmosphere to space: present-day loss rates determined from MAVEN observations and integrated loss through time. *Icarus* **315**, 146–157 (2018).
23. Wang, J. et al. MAVEN observations of magnetic reconnection at Martian induced magnetopause. *Geophys. Res. Lett.* **48**, e2021GL095426 (2021).
24. Xu, X. et al. Ion loss within a reconnection exhaust near Mars: MAVEN observations. *Astrophys. J.* **955**, 41–46 (2023).
25. Jakosky, B. M. et al. The Mars Atmosphere and Volatile Evolution (MAVEN) mission. *Space Sci. Rev.* **195**, 3–48 (2015).
26. Morschhauser, A., Lesur, V. & Grott, M. A spherical harmonic model of the lithospheric magnetic field of Mars. *J. Geophys. Res. Planets* **119**, 1162–1188 (2014).
27. Sonnerup, B. U. Ö. & Cahill, L. J. Magnetopause structure and attitude from Explorer 12 observations. *J. Geophys. Res.* **72**, 171–183 (1967).
28. Sonnerup, B. U. & Scheible, M. in *Analysis Methods for Multi-Spacecraft Data* (eds Paschmann, G. & Daly P.W.) (ESA Publications, 1998).
29. Brain, D. A., Lillis, R. J., Mitchell, D. L., Halekas, J. S. & Lin, R. P. Electron pitch angle distributions as indicators of magnetic field topology near Mars. *J. Geophys. Res.* **112**, A09201 (2007).
30. Mitchell, D. G. et al. An extended study of the low-latitude boundary layer on the dawn and dusk flanks of the magnetosphere. *J. Geophys. Res.* **92**, 7394–7404 (1987).
31. Xu, S. et al. Martian low-altitude magnetic topology deduced from MAVEN/SWEA observations. *J. Geophys. Res. Space Phys.* **122**, 1831–1852 (2017).
32. Xu, S. et al. A technique to infer magnetic topology at Mars and its application to the terminator region. *J. Geophys. Res. Space Phys.* **124**, 1823–1842 (2019).
33. Priest, E. & Forbes, T. *Magnetic Reconnection: MHD Theory and Applications* (Cambridge Univ. Press, 2000).

34. Burch, J. L. & Phan, T. D. Magnetic reconnection at the dayside magnetopause: advances with MMS. *Geophys. Res. Lett.* **43**, 8327–8338 (2016).
35. Øieroset, M., Phan, T. D., Fujimoto, M., Lin, R. P. & Lepping, R. P. In situ detection of collisionless reconnection in the Earth's magnetotail. *Nature* **412**, 414–417 (2001).
36. Gosling, J. T. Magnetic reconnection in the solar wind. *Space Sci. Rev.* **172**, 187–200 (2011).
37. Xu, X. et al. ARTEMIS observations of well-structured lunar wake in subsonic plasma flow. *Astrophys. J.* **881**, 76 (2019).
38. Jr, E. W. H. Magnetic reconnection in the Earth's magnetotail. *Aust. J. Phys.* **38**, 981–998 (1985).
39. Gosling, J. T., Birn, J. & Hesse, M. Three-dimensional magnetic reconnection and the magnetic topology of coronal mass ejection events. *Geophys. Res. Lett.* **22**, 869–872 (1995).
40. *Planetary Data System* (NASA, 2024); https://pds.nasa.gov
41. *MAVEN Science Data Center* (Laboratory for Atmospheric and Space Physics, University of Colorado, 2024); https://lasp.colorado.edu/maven/sdc/public/
42. Ye, Y. *MAVEN Data Supplementary Toolkit* (GitHub, 2024); https://github.com/StellarPlasma/MAVEN_IDL
43. SPEDAS (The Space Physics Environment Data Analysis Software, 2024); http://spedas.org/wiki/index.php?title=Downloads_and_Installation
44. Coates, A. J. et al. Ionospheric photoelectrons: comparing Venus, Earth, Mars and Titan. *Planet. Space Sci.* **59**, 1019–1027 (2011).

Acknowledgements

This work is funded by the National Natural Science Foundation of China (NSFC) under grants 42122061 and 42241112, the Science and Technology Development Fund, Macau SAR (file nos. 0098/2022/A2 and 0003/2022/AFJ), the Macau Foundation and the National Science and Technology Council in Taiwan under grant NSTC 112-2111-M-002-019. We acknowledge the MAVEN contract for their support and the MAVEN-STATIC instrument team for their assistance in interpreting the data. All MAVEN data are available on the Planetary Data System (https://pds.nasa.gov). The funds (grants and first author) were as follows: grant 42122061, National Natural Science Foundation of China (X.X.); grant 42241112, National Natural Science Foundation of China (X.X.); no. 0098/2022/A2, Science and Technology Development Fund, Macau SAR (X.X.); no. 0003/2022/AFJ, Science and Technology Development Fund, Macau SAR (X.X.); grant NSTC 112-2111-M-002-019, National Science and Technology Council in Taiwan (L.-C.L.).

Author contributions

Y.Y. carried out the analysis. X.X. proposed the concept of ionospheric mass ejection at Mars, identified the mass ejection event and led the group. Y.Y. and X.X. drafted the manuscript. L.C.L. participated in the interpretation of the data, and J.Y. participated in the data processing. All authors discussed the results and commented on the paper.

Competing interests

The authors declare no competing interests.

Additional information

Supplementary information The online version contains supplementary material available at https://doi.org/10.1038/s41550-024-02254-3.

Correspondence and requests for materials should be addressed to Xiaojun Xu or Lou-Chuang Lee.

Peer review information *Nature Astronomy* thanks Thomas Cravens and the other, anonymous, reviewer(s) for their contribution to the peer review of this work.